A High-Quality Three-Phase Rectifier complying with IEC 61000-3-4 Standards

Joanna A. G. Marafão, José Antenor Pomilio
School of Electrical and Computer Engineering, University of Campinas
C. P. 6101 13081-970 Campinas – BRAZIL
e-mail: antenor@dsce.fee.unicamp.br

Giorgio Spiazzi
Dept. of Electronics and Informatics - University of Padova (Italy)
Via Gradenigo 6/a, 35131 Padova - ITALY
E-mail: spiazzi@dei.unipd.it

Abstract – A high-quality three-phase diode rectifier, based on a conventional rectifier with an add-on simple cell with line-frequency commutated AC switches is presented in this paper. The boost action introduced by the commutation cell allows for a complete compensation of the voltage drop across the input inductors. Moreover, as compared to other line-frequency commutated rectifiers, the proposed circuit allows compliance with the low-frequency harmonic limits defined in the technical report IEC 61000-3-4 for any power range. High-efficiency and minimum EMI are obtained due to the low-frequency commutations. A converter prototype was built and tested. The results confirm the theoretical analysis.

I. INTRODUCTION

Three-phase Diode Bridges are extensively used in many high-power low-cost applications leading the degradation in the power quality due to the current distortion. In the attempt to reduce their effects, various standard and recommendations have been introduced in order to limit the harmonics that an individual load can inject into the utility. Recently, the Technical Report IEC 61000-3-4 was issued with the intent to extend the field of application of standard IEC 61000-3-2 for electrical and electronic equipment with a rated input current exceeding 16 A per phase [1].

Many solutions have been proposed [2-5] using passive or active approaches, these last employing high or low frequency commutation. Passive filters, besides do not allow the regulation of the output voltage, decrease its value in comparison with the unfiltered rectifier. Taking the harmonic limits as a quality index, the resulting inductors are typically larger than the ones used in high-quality rectifiers using active circuits.

It is well known that a PWM rectifier is able to establish a phased sinusoidal current. For this purpose it is necessary a fully controlled rectifier, that generates EMI and decreases the overall efficiency due the high frequency commutation.

Low-frequency commutation topologies are a trade-off between the passive and the high-frequency solutions, allowing to get a low-distortion input current, relatively small passive components, minimum losses end practically no EMI.

Such approach is proposed in [4], where three low-power line-frequency commutated switches and three line inductors are employed in order to reduce the input current distortion of three-phase diode rectifiers with a capacitive filter. The circuit feature low-cost, simplicity, high efficiency and low EMI.

In this paper a similar structure is proposed in which the input inductors are allowed to resonate with the dc link capacitors, thus adding some good features to the original converter [4]. Increases the boost action, which allows for a complete compensation of the voltage drop across the input inductors, from no-load to full-load and reduces input current harmonic content, thus complying with IEC 61000-3-4 limits at any power level.

In section II, the converter behavior is analyzed in detail and expressions for input current waveforms are derived, in section III the input current harmonic content is calculated while in section IV suitable design criteria are given. Measurements on an experimental prototype are reported in section V, showing a good agreement with the theoretical analysis.

II. CONVERTER ANALYSIS

The proposed three-phase high-quality rectifier is shown in Fig. 1.

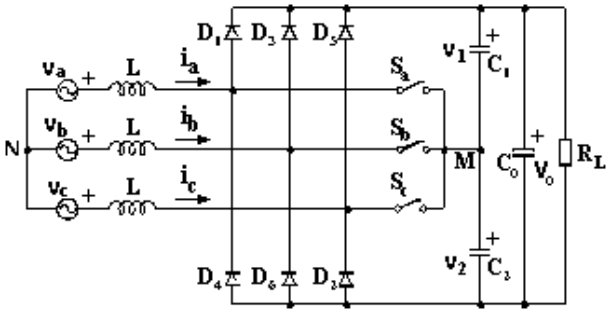

Fig. 1 - Scheme of the proposed three-phase high-quality rectifier.

As we can see, it is formally topologically similar to the Vienna rectifier (but in this case the switches commutate at low frequency) and to the rectifier presented in [4], the main difference is the reduced value of the output capacitors C_1 and C_2, which allows for the resonance between input inductor and these capacitors to occur during each switch turn-on interval. This resonance, substantially improves the input current waveforms, and introduces a new degree of freedom in the converter design, as compared to the original topology. S_a, S_b, S_c are bi-directional switches which can

be built by using one switch and a diode bridge rectifier each. All these components are commutated at the line frequency, what reduces EMI and losses and allows for the utilization of slow devices, thus saving cost and improving converter reliability. Moreover, the input inductors are standard line-frequency iron-core low-cost inductors.

In the following, the input current and capacitor voltage waveforms are calculated in the line half period, assuming the following conditions:

- balanced three-phase input voltages;
- voltages v_1 and v_2 across the two resonant capacitors C_1 and C_2 satisfying the following inequality: $0 < v_1, v_2 < V_o$;
- constant output voltage V_o;
- synchronized switch turn on with zero crossing of the corresponding phase voltage;
- switch turn on interval equal to $T_i/12$ (T_i is the line period).

The phase voltage v_a and phase current i_a, are is shown in Fig. 2.

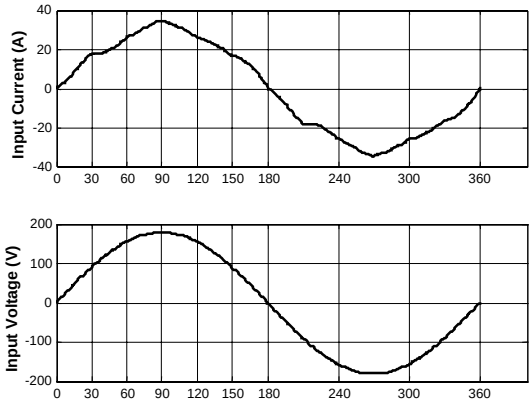

Fig. 2. Current and Voltage phase a in a line period.

The gate signals sequence is shown in Fig. 3, together with a capacitor voltages v_1 and v_2. The line half period is subdivided into six intervals which are indicated by the value of the line angle $\theta = \omega_i t$, as shown in Fig. 2. The topological sequence, and the equations describing normalized phase current i_{aN} [7] are shown in the Annex I, at the end of the paper.

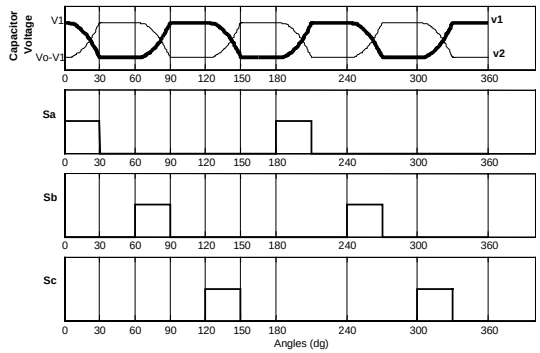

Fig. 3 - Capacitor voltages v_1 and v_2, and drive signal patterns in a line period.

The following base variables have been used for normalization:

Base voltage: $V_N = V_{pk}$ (1.a)

Base current: $I_N = \dfrac{V_{pk}}{\omega_i L}$ (1.b)

Base power: $P_N = V_N I_N = \dfrac{V_{pk}^2}{\omega_i L}$. (1.c)

The other parameters used in the equations are ($C=C_1=C_2$):

Resonant angular frequency: $\omega_o = \dfrac{1}{\sqrt{3LC}}$

Normalized resonant frequency: $\alpha = \dfrac{\omega_o}{\omega_i}$

Voltage conversion ratio: $M(\alpha) = \dfrac{V_o}{V_{pk}}$

Adimensional parameter: $K(\alpha) = \dfrac{\dfrac{\alpha}{2} - sin\left(\alpha\dfrac{\pi}{6}\right)}{1+\cos\left(\alpha\dfrac{\pi}{6}\right)}$

The expression for the voltage conversion ratio $M(\alpha)$ used in these equations is derived by imposing a zero value for the current at the end of the line half period. The result is the following relation:

$$M(\alpha) = \frac{18}{7\pi}\left\{1 + \frac{\sqrt{3}}{2}\frac{\alpha^2}{\alpha^2-1} - \frac{1}{\alpha^2-1}\left[\cos\left(\alpha\frac{\pi}{6}\right) - K(\alpha)sin\left(\alpha\frac{\pi}{6}\right)\right]\right\} \quad (2)$$

while the expression for the initial voltage value across C_1, denoted V_1 in Fig. 3, derived by letting $v_1(\pi/6)=(V_o-V_1)$, is given by:

$$V_{1N} = \frac{M(\alpha)}{2} + \frac{3}{2}\frac{\alpha}{\alpha^2-1}K(\alpha) \quad (3)$$

As we can see, the voltage conversion ratio together with the phase current waveforms, depend only on the normalized resonant frequency α.

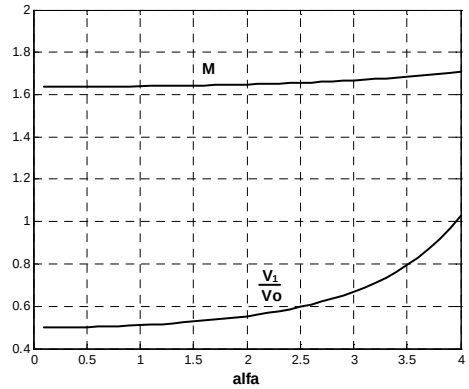

Fig. 4 - Voltage conversion ratio M and initial capacitor voltage V_1 normalized to the output voltage V_o as a function of normalized resonant frequency α.

Fig. 4, reports the voltage conversion ratio M and the initial capacitor voltage V_1 normalized to the output voltage V_o as a function of parameter α (note that $V_1/V_o = V_{1N}/M$). The value of the theoretic voltage conversion

ratio of a standard three-phase diode bridge rectifier without input inductances given by:

$$M_T = \frac{V_{oT}}{V_{gpk}} = \frac{3}{\pi}\sqrt{3} = 1.654$$

To the purpose of comparison, the original converter [4] was able to achieve a voltage conversion ratio equal to 1.637, which correspond exactly to the value that tends expression (2) for α approaching zero. In fact, when the value of capacitors C_1 and C_2 is chosen high enough so as to keep their voltage constant and equal to $V_o/2$, the converter behaves in the same manner as the original one, and the resonant frequency becomes very low (see also in Fig. 4 the voltage V_1/V_o tends to 1/2 at low α values). Thus, the proposed converter provides enough boost action so as to completely compensate for the voltage drop across the input inductors. This means that it is possible to maintain the output voltage constant from no load to full load simply reducing the on-time of switches S_a, S_b and S_c.

From Fig. 4 we can also see that the maximum voltage conversion ratio is limited by the value of parameter α that causes a complete swing of voltages v_1 and v_2 from zero to V_o. Such value can be derived by setting $V_{1N} = M$ in (3), or $V_1/V_o = 1$. The result is $\alpha_{max} = 3.952$ (see Fig. 4). The maximum voltage conversion ratio results $M_{max} = 1.7$. For a higher value of parameter α the current distortion increases, as shown in Fig. 5, so as a good design should select $\alpha<\alpha_{max}$.

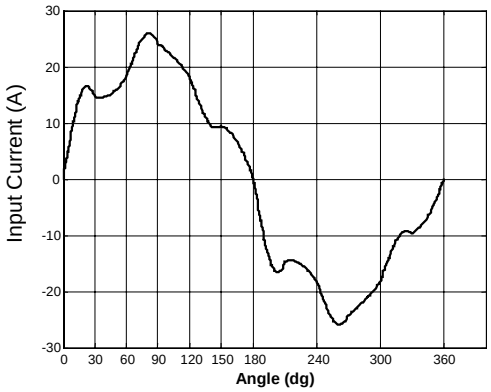

Fig. 5 – Current distortion for $\alpha = 4.4$.

Since the input current waveform depends only on parameter α, we can choose the input inductance value based only on the desired output power. In fact, the three-phase average input power is:

$$P_{in} = \frac{3}{\pi}\int_0^{\pi} v_a(\theta) i_a(\theta)\, d\theta = \frac{V_{pk}^2}{\omega_i L}\frac{3}{\pi}\int_0^{\pi} v_{aN}(\theta) i_{aN}(\theta)\, d\theta = \frac{V_{pk}^2}{\omega_i L} P_{inN} \quad (4)$$

Where P_{inN} is the normalized average input power, which is shown in Fig. 6 as a function of parameter α. As we can see, the resonant intervals give a power gain, as compared to the original solution with constant capacitor voltages, which can be as high as 36.4% ($P_{in}(0) = 0.391$, $P_{in}(\alpha_{max}) = 0.533$).

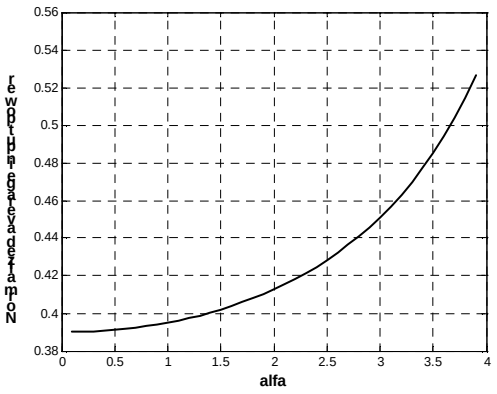

Fig. 6 – Normalized average input power as a function of parameter α

III. Input Current Analysis

The major claimed benefit of the proposed converter, as compared to the original one, is the reduction of the input current harmonic content. Since the proposed converter is suitable for high power applications, we will take as reference the harmonic limits described in the technical report IEC 61000-3-4: "*Limitation of emission of harmonic currents in low-voltage power supply systems for equipment with rated current greater than 16 A per phase*".

In particular, the limits are those called "stage 1: current emission values for simplified connection of equipment ($S_{equ} \le S_{sc} / 33$)", and are reported in Table I. As we can see, each harmonic current limit is specified as a function of the rated fundamental current (up to the 40th harmonic). This fact allows analyzing the converter input current harmonics independently of the input power.

Table I - Limits of technical report IEC 61000-3-4: "Stage1: current emission values for simplified connection of equipment ($S_{equ} \le S_{sc}/33$)"

Harmonic number n	Admissible harmonic current $\mathbf{I_n/I_1^*}$ %	Harmonic number n	Admissible harmonic current $\mathbf{I_n/I_1^*}$ %
3	21.6	21	≤ 0.6
5	10.7	23	0.9
7	7.2	25	0.8
9	3.8	27	≤ 0.6
11	3.1	29	0.7
13	2	31	0.7
15	0.7	≥ 33	≤ 0.6
17	1.2		
19	1.1	Even	≤ 8/n or ≤ 0.6

As already observed in the previous sections, the input current waveform depends only on the value of the normalized resonant frequency α. Thus, an analysis was performed in order to calculate the current harmonic amplitudes at different α values. The results are reported in Fig. 7 (unity fundamental component), together with limit values L5, L11, L13 corresponding to 5a, 11a, 13a harmonics limits (all the others are outside the graph scale). It is worth to remember that, as stated in the technical report, all harmonics having amplitude lower than 0.6% of the rated fundamental component can be

disregarded. Thus, the 17[a], 19[a] and above 25[a] can be always neglected, no matter the value of α is. Another interesting results is that the original converter does not comply with these limits, at any output power, since 11[a] and 13[a] harmonics exceed their limits. The minimum value of α needed to comply with the standard is 1.95.

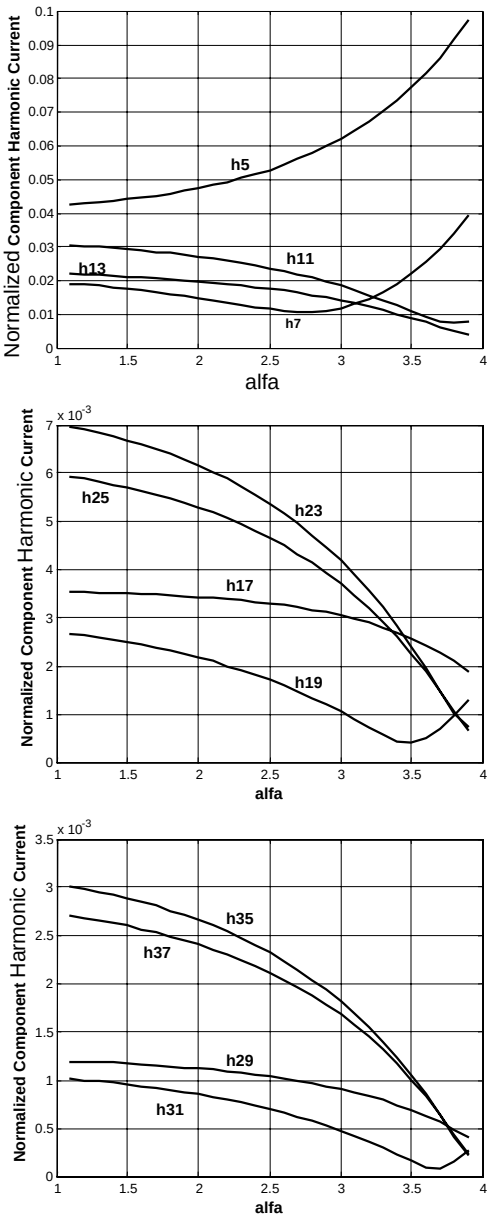

Fig. 7 – Simulated input current harmonic amplitudes as a function of normalized resonant frequency α (unity fundamental component).

IV. Design Example

In this section we report the design example of a converter having the following specifications:

Input voltage:..... V_{in}= 127V_{rms}

Output power:..... P_o= 9.5kW

Estimated converter efficiency: ..... η= 1

The efficiency was considered unity to allow a comparison of theoretical expectations with simulation results.

The design procedure is as follows:

1. Choose a suitable value of α greater than α_{min}. This is necessary to comply with the technical report IEC61000-3-4, also at a reduced load power. In order to keep the output voltage constant, it is necessary to reduce the switch on-time, causing an increase in the input current distortion.
2. Calculate the input inductance value needed for the specified input power $P_{in} = P_o/\eta$ using (4) and Fig. 6.
3. Calculate the resonant capacitor from the knowledge of parameters α and L, using the definition of α and ω_o.
4. Verify the input current harmonic content at lower output power levels.

We choose α=3.6, higher than α_{min}. From (2) and (3) the output voltage turns out to be 303V. From (4), the input inductance value needed to achieve the desired power is L=4.5mH, and from the definition of α and ω_o, the output capacitor values result C=40μF.

The simulation, at nominal conditions, gives an average output voltage of 299,5V (output filter capacitor C_o=600μF), and the input current spectrum shows a very good agreement with the calculated one.

At nominal power level, it is possible to keep the output voltage constant only for input over voltage situations. In this case the switches on-time must be reduced decreasing the boost effect. It is not possible compensation for input under-voltages

Eventually some harmonics can be above the limits but the measurement test applies only for the rated voltage.

Simulations have been performed in order to verify the input current harmonic content at different power levels (keeping the output voltage constant).

The control strategy delays the switches command with respect to the phase voltage zero crossing, while keeping constant their turn-off instant.

The results are shown in Fig. 8. A higher value of α, as compared to the minimum value, based only on nominal conditions, is necessary to maintain the harmonic amplitudes below the limits from no load to full load.

For the example, I_1 = 32,33A (corresponding to 9650W), only harmonics 5[th], 7[th], 11[th], 13[th], and 17[th], have to be considered. As we can see the harmonic closest to the limit is the 11[th], at 6kW (I_{13} = 0.951 A as compared to I_{13LIM} = 1 A).

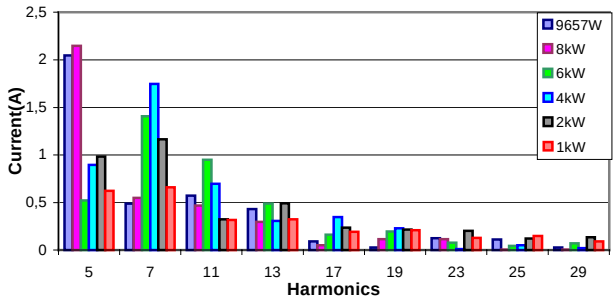

Fig. 8 – Input current harmonic amplitudes at different power levels

V. Experimental Results

An 8.5 kW prototype was built with following specifications: Input voltage 127V; Inductance: 4.5 mH, Capacitors: 60 μF (α=2.95), Output Capacitor: 600 μF, Output voltage: 300V.

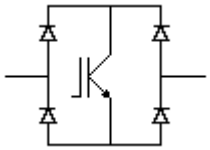

Fig. 9 – Bi-directional switch used in the prototype.

Each of the bi-directional switches Sa, Sb and Sc was assembled with IRG4PC50UD IGBT connected between the DC nodes of a rectifier bridge, SKB 15/04 Semikron, as shown in fig. 9. As three-phase diode bridge, SKD 50/12 Semikron was used.

The waveforms are shown in Fig. 10. The measured power factor is 0.994 and the output voltage 295V. The efficiency at rated power is 93%. The current spectrum is shown in Fig. 11. The closest components are the 11th and the 13th. The higher components do not reach the 0.6% limit.

For comparison purposes, Fig. 12 shows the input current without the action of the auxiliary circuit. The output voltage decreases to 253V, the power factor is 0.88, and the available output power is 5.9 kW.

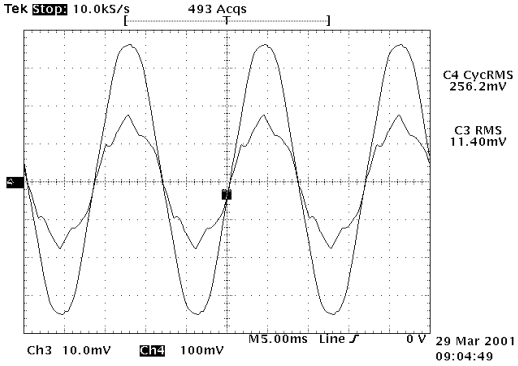

Fig. 10 – Input voltage (100V/div.) and current (20A/div.)

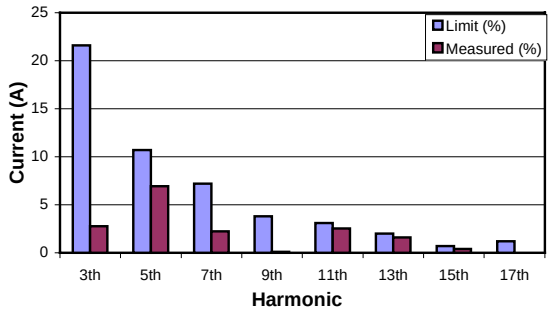

Fig. 11 – Current spectrum at rated power.

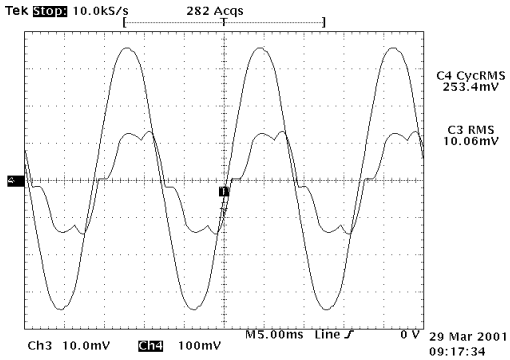

Fig. 12 – Input voltage (100V/div.) and current (20A/div.) with passive filter.

VI. Conclusions

The proposed add-on circuit is able to compensate for current distortion produced by diode bridge rectifiers with capacitive filter. The resulting current harmonics are below the limits of IEC 61000-3-4 for any power level. It is possible to compensate for input over-voltage by adjusting the auxiliary switches signals. The use of low-frequency commutation minimizes losses, thus increasing the overall efficiency. The inductance value is reduced as compared to the purely passive circuit. The experimental results confirm the circuit behavior.

Acknowledgement

The authors would like to acknowledge the Fundação de Amparo à Pesquisa do Estado de S. Paulo by the support of this project.

References

[1] Commission Electrotechnique Internationale, IEC 61000-3-4, "Limitation of emission of harmonic currents in low-voltage power supply systems for equipment with rated current greater than 16 A per phase", 3, rue de Varembé, Genève, Switzerland, 1998.

[2] F. Z. Peng, G-J Su and G. Farquharson: "A series LC filter for harmonic compensation of AC drives", CD-ROM of IEEE PESC'99, 1999.

[3] A. R. Prasad, P. D. Ziogas and S. Manias: "An active Power Factor Correction Technique for Three-Phase Diode Rectifier". IEEE PESC '89 Record, pp. 58-66.

[4] E. L. M. Mehl, I. Barbi, "An Improved High-Power Factor and Low-Cost Three-Phase Rectifier," IEEE Trans. On Industry Applications, Vol. 33, NO.2, March/April, 1997, pp. 485-492.

[5] S. Hansen, P. N. Enjeti, J-H. Hahn, F. Blaabjerg, "An integrated single-switch approach to improve harmonic performance of standard PWM adjustable-speed drives", IEEE Trans. On Industry Applications, Vol. 36, NO.4, July/August, 2000, pp. 1189-1196.

[6] J. A. Pomilio, G. Spiazzi, "A Double-Line-Frequency Commutated Rectifier Complying with IEC 1000-3-2 Standards", IEEE Applied Power Electronics Conf. Proc. (APEC), March, 1999, pp. 349-355.

[7] J. A. G. Marafao, J. A. Pomilio, G. Spiazzi "Improved Three-Phase High-Quality Rectifier with Line-Commutated Switches", IEEE Power Electronics Spec. Conf. (PESC), June 2001.

Annex 1 - Equations describing phase current i_a and capacitor voltage u_2 in a line half period

Interval	Fundamental equations
$0 \le \theta \le 30°$	$i_{aN}(\theta)=\frac{1}{\alpha^2-1}[\cos(\theta)-\cos(\alpha\theta)+K(\alpha)\sin(\alpha\theta)]$, $u_{2N}(\theta)=\frac{M(\alpha)}{2}+\frac{3}{2}\frac{\alpha}{\alpha^2-1}[\alpha\sin(\theta)-\sin(\alpha\theta)-K(\alpha)\cos(\alpha\theta)]$ $I_{a1N}=\frac{1}{\alpha^2-1}\left[\frac{\sqrt{3}}{2}-\cos\left(\alpha\frac{\pi}{6}\right)+K(\alpha)\sin\left(\alpha\frac{\pi}{6}\right)\right]$
$30° \le \theta \le 60°$	$i_{aN}(\theta)=I_{a1N}+\frac{\sqrt{3}}{2}-\cos(\theta)-\frac{M(\alpha)}{3}\left(\theta-\frac{\pi}{6}\right)$, $u_{2N}(\theta)=U_{1N}$, $I_{a2N}=I_{a1N}+\frac{\sqrt{3}-1}{2}-M(\alpha)\frac{\pi}{18}$
$60° \le \theta \le 90°$	$i_{aN}(\theta)=I_{a2N}+\frac{\alpha^2}{2(\alpha^2-1)}\cos\left(\theta-\frac{\pi}{3}\right)-\cos(\theta)-\frac{M(\alpha)}{2}\left(\theta-\frac{\pi}{3}\right)-\frac{1}{2(\alpha^2-1)}\left[\cos\left(\alpha\left(\theta-\frac{\pi}{3}\right)\right)-K(\alpha)\sin\left(\alpha\left(\theta-\frac{\pi}{3}\right)\right)\right]$ $u_{2N}(\theta)=\frac{M(\alpha)}{2}-\frac{3}{2}\frac{\alpha}{\alpha^2-1}\left[\alpha\sin\left(\theta-\frac{\pi}{3}\right)-\sin\left(\alpha\left(\theta-\frac{\pi}{3}\right)\right)-K(\alpha)\cos\left(\alpha\left(\theta-\frac{\pi}{3}\right)\right)\right]$ $I_{a3N}=I_{a2N}-M(\alpha)\frac{\pi}{12}-\frac{1}{2(\alpha^2-1)}\left[\cos\left(\alpha\frac{\pi}{6}\right)-K(\alpha)\sin\left(\alpha\frac{\pi}{6}\right)-\alpha^2\frac{\sqrt{3}}{2}\right]$
$90° \le \theta \le 120°$	$i_{aN}(\theta)=I_{a3N}-\cos(\theta)-\frac{2}{3}M(\alpha)\left(\theta-\frac{\pi}{2}\right)$, $u_{2N}(\theta)=U_{oN}-U_{1N}$, $I_{a4N}=I_{a3N}+\frac{1}{2}-M(\alpha)\frac{\pi}{9}$
$120° \le \theta \le 150°$	$i_{aN}(\theta)=I_{a4N}-\frac{\alpha^2}{2(\alpha^2-1)}\cos\left(\theta-\frac{2\pi}{3}\right)-\cos(\theta)-\frac{M(\alpha)}{2}\left(\theta-\frac{2\pi}{3}\right)+\frac{1}{2(\alpha^2-1)}\left[\cos\left(\alpha\left(\theta-\frac{2\pi}{3}\right)\right)-K(\alpha)\sin\left(\alpha\left(\theta-\frac{2\pi}{3}\right)\right)\right]$ $u_{2N}(\theta)=\frac{M(\alpha)}{2}+\frac{3}{2}\frac{\alpha}{\alpha^2-1}\left[\alpha\sin\left(\theta-\frac{2\pi}{3}\right)-\sin\left(\alpha\left(\theta-\frac{2\pi}{3}\right)\right)-K(\alpha)\cos\left(\alpha\left(\theta-\frac{2\pi}{3}\right)\right)\right]$
$150° \le \theta \le 180°$	$i_{aN}(\theta)=I_{a5N}-\frac{\sqrt{3}}{2}-\cos(\theta)-\frac{M(\alpha)}{3}\left(\theta-\frac{5\pi}{6}\right)$, $u_{2N}(\theta)=U_{1N}$, $I_{a6N}=0$ $I_{a5N}=I_{a4N}-M(\alpha)\frac{\pi}{12}+\frac{1}{2(\alpha^2-1)}\left[\cos\left(\alpha\frac{\pi}{6}\right)-K(\alpha)\sin\left(\alpha\frac{\pi}{6}\right)+(\alpha^2-2)\frac{\sqrt{3}}{2}\right]$